Discrete Periodic Melting Point Observations for Nanostructure Ensembles

M. Yu. Efremov,[1] F. Schiettekatte,[1] M. Zhang,[1] E. A. Olson,[1] A. T. Kwan,[1] R. S. Berry,[2] and L. H. Allen[1,*]

[1]*Material Science and Engineering Department and Coordinated Science Laboratory, University of Illinois at Urbana-Champaign, Urbana, Illinois 61801*

[2]*Department of Chemistry, University of Chicago, Chicago, Illinois 60637*

(Received 31 May 2000)

We report a study of the thermodynamic properties of indium clusters on a SiN_x surface during the early stages of thin film growth using a sensitive nanocalorimetry technique. The measurements reveal the presence of abnormal discontinuities in the heat of melting below 100 °C. These discontinuities, for which temperature separation corresponds to a spatial periodicity equal to the thickness of an indium monolayer, are found to be related to the atomic "magic numbers," i.e., the number of atoms necessary to form a complete shell of atoms at particle surface.

PACS numbers: 05.70.Fh, 65.20.+w, 65.40.+g, 65.50.+m

The next millennium will be marked by major advances in materials and biology, spearheaded in part by the gains made in manipulating and characterizing materials on the nanometer scale. Materials of nanometer dimensions have unusual thermodynamic properties that are of great appeal for both scientific and technology communities [1–5]. Two phenomena which are currently of intense interest include (a) discrete nature of nanostructures and clusters which show periodic variations in properties corresponding to some select number of atoms ("magic" numbers) and (b) size-dependent melting point depression of small particles. This area of research is of particular interest in microelectronics for the study of the initial stages of thin film growth.

The discrete nature of nanostructures has been observed with clusters deposited on surfaces as well as clusters in beams. It is shown that two-dimensional iridium clusters of specific integral sizes (e.g., $Ir_{19}, Ir_{37}, \ldots$) on a surface are considerably more stable than clusters with fewer or greater numbers of atoms [6]. In cluster beams certain cluster sizes also show enhanced stability, which have been experimentally observed for clusters with a few atoms up to 22 000 atoms [7].

Size-dependent melting point depression is an important phenomenon for particles of size less than 10 nm. This is due to the increased influence of the surface atoms as the ratio of surface/bulk atoms increases. As the particle size decreases, the value of the melting point decreases from the bulk value. Size-dependent melting point depression has been confirmed experimentally over a broad range of particle sizes by using a variety of methods [transmission electron microscopy (TEM) [8], x-ray diffraction (XRD) [9], and differential scanning calorimetry [10]] for particles in cluster beams [11–14] as well as those on surfaces [8,15]. TEM and XRD measure the melting temperature by monitoring the loss of crystalline structure of the particles with increasing temperature. On the other hand, calorimetric techniques measure the heat involved in the melting process as a function of the temperature.

Recent improvements in nanocalorimetry, which was developed in our laboratory, allow us to measure the melting point depression for particles on surfaces having only 1000 atoms. At this level of size, small changes in the particle size correspond to large changes in melting point which are easily measured with our nanocalorimeter. Thus we can investigate from the energetic point of view the discrete nature of nanostructures with sizes in the range of 1000 to 10 000 atoms by measuring the heat capacity of the particles.

In this Letter, we report observations of multiple periodic maxima (melting peaks) in heat capacity measurement of particles in the range of 2–4 nm. These oscillating maxima correspond to particle sizes, which differ incrementally in radius by one atomic monolayer (2.4 Å). These results clearly show the enhanced stability of particles of certain radii as their melting temperature decreases with their size.

The nanostructures studied in this work were formed by thermal evaporation of indium onto the SiN_x membrane surface of the nanocalorimeter (see Fig. 1). For the

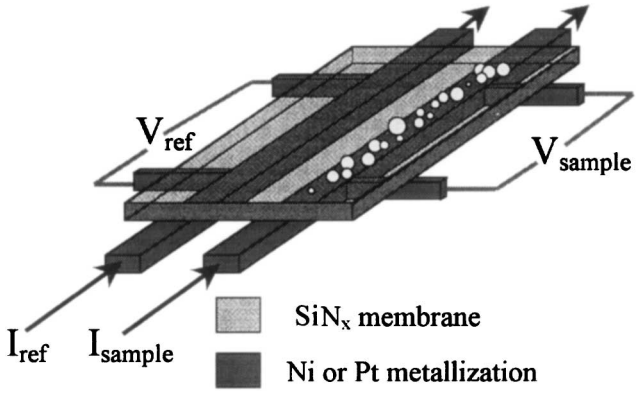

FIG. 1. The schematic diagram of the nanocalorimeter showing two metallic strips, which serve as both heaters (sample and reference) and thermometers. These strips are supported by a thin SiN_x membrane. Indium is deposited on the membrane side of the nanocalorimeter directly above the sample heater.

 0031-9007/00/85(17)/3560(4)$15.00

very small amounts of indium which were deposited for this study, the films were discontinuous [16], consisting of self-assembled nanostructure with radii of a few nm. The deposition pressure was 1×10^{-8} Torr and no evidence of oxidation of the nanoparticles was observed.

The nanocalorimetry technique used for this study is based on devices which have been developed during the last several years [15,17–19]. The device shown in Fig. 1 consists of a thin, 30 nm SiN_x membrane typically several millimeters wide. Two metallic strips (Ni, Au, or Pt) with a width of 400 μm and 50 nm thick are deposited onto the one side of the membrane, and serve both as heaters and as resistive thermometers [20]. By using a thin SiN_x membrane as the support system [21] the sensor has exceptionally low mass addenda. The resistivity of the heater is carefully calibrated against temperature prior to the experiments. Very fast heating rates (up to 10^6 K/s) have been achieved by this method, making the radiative and conductive losses negligible. The calorimetric cell (which includes the metal strip, the indium film, and the part of the SiN_x membrane between them) is thus operated under nearly adiabatic conditions. Calorimetric measurements are performed in differential mode where one of the metal strips serves as the reference sensor. The indium is deposited directly on the SiN_x, aligned with one of the metal strips, which serves as the sample heater. Calorimetric measurements are performed *in situ*, and proceed by applying a current pulse to both sample and reference metal strips simultaneously. The voltage and current across the heaters are measured and used for power, temperature, and heat capacity calculations. The device also serves as the TEM sample since the SiN_x membrane is nearly transparent.

After indium deposition, the calorimeters are scanned to 300 °C in order to anneal the particles and make them stable. Then, the calorimetric measurements are performed. Calorimetric data are presented as a relation between the heat capacity of sample C_P and the sample temperature T. Each $C_P(T)$ curve presented here is an average of 100 scans, in order to increase the sensitivity. Nevertheless, the features discussed are observable in each single scan.

Typically the $C_P(T)$ relation for melting of small particles deposited on a free surface has a single broad endothermic "melting" peak [18]. The area under this peak is equal to the total latent heat of fusion of the particles. The wide size distribution of the deposited particles causes broadening of the melting peak because each particle of a different size melts at a different temperature—a consequence of size-dependent melting point depression.

However, for the smaller indium clusters (2–4 nm), a remarkable effect is observed. The calorimetric curve shows a series of peaks in the low temperature tail, starting at 100 °C down to 50 °C. $C_P(T)$ data for the 0.4, 0.6, and 0.8 nm indium films are presented in Fig. 2(d). Only three

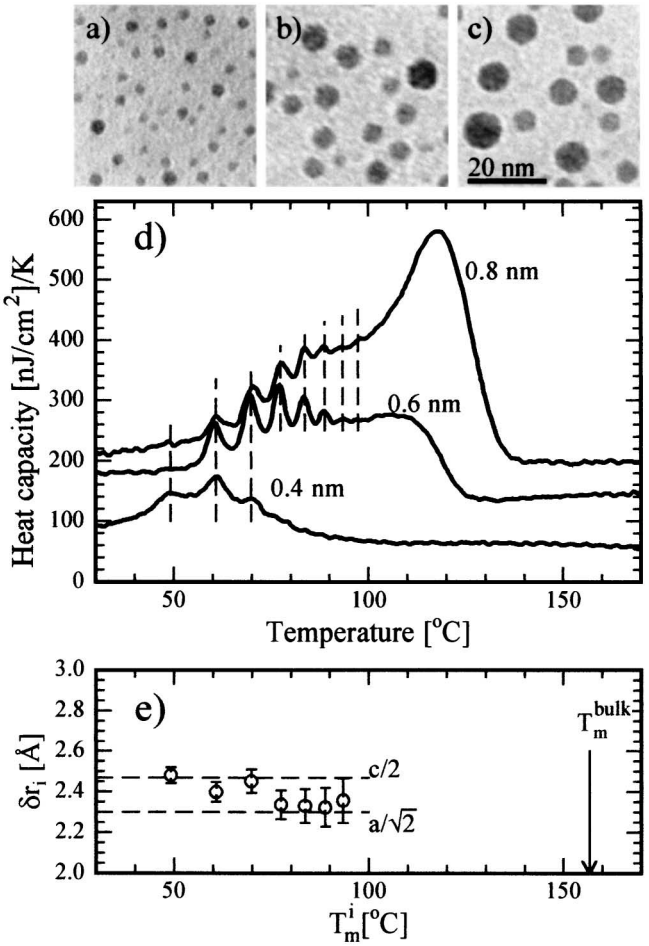

FIG. 2. *Ex situ* TEM micrographs of the nanoparticles generated in the deposition experiments of the (a) 0.4 nm, (b) 0.6 nm, and (c) 0.8 nm films. Corresponding calorimetric curves (d) with the vertical dashed lines indicating the position in temperature of each maximum. (e) Radius difference corresponding to the separation between adjacent maxima, as calculated using Eq. (2). The horizontal dashed lines represent the thickness of a monolayer for the two bulk lattice parameters of indium.

peaks are present for the 0.4 nm deposition, but after an additional 0.2 nm indium is deposited (increasing the average size of particles in the distribution), we find an additional five peaks generated in the $C_P(T)$ data. It is seen that the position of the peaks with respect to temperature is fixed from one deposition step to the other. Furthermore the peaks persist independently of the heating rate (3×10^4–2×10^5 K/s) and the type of calorimeter (nickel or platinum metallization, and nanocalorimeters with various dimensions).

To quantitatively relate the temperature of the peaks to a specific size of nanostructures we utilize the experimental relationship between size and melting point as derived from our previous work [22]. As is the case of many material systems documented in the literature, indium nanoparticles show a proportional relation between their melting point depression ΔT_m and their curvature

(i.e., reciprocal radius r^{-1}) over a broad range of size (down to 2 nm of radius),

$$\Delta T_m = T_m^{\text{bulk}} - T_m = \frac{\alpha}{r}, \quad (1)$$

where T_m is the melting temperature of an indium particle with radius r and T_m^{bulk} is the melting temperature of bulk indium, 429.75 K. The slope $\alpha = 220 \pm 10$ nm K has been determined experimentally [22]. Equation (1) corresponds to the widely used homogeneous melting model [23], which is based on Laplace and Gibbs-Duhem equations. According to Eq. (1), a melting temperature between 40 °C and 100 °C corresponds to particles with radii between 2 and 4 nm.

Key information regarding these oscillations is extracted by analyzing the temperature spacing of the peaks, which increases with decreasing temperature. We evaluate these oscillations by relating their temperature to their radius through Eq. (1). The radius difference $\delta r_i = r_{i+1} - r_i$ which corresponds to the separation between a maximum T_m^i and the next T_m^{i+1} is given by

$$\delta r_i = \frac{\alpha (T_m^{i+1} - T_m^i)}{(T_m^{\text{bulk}} - T_m^i)(T_m^{\text{bulk}} - T_m^{i+1})}. \quad (2)$$

The result of this calculation, using the values found for the different maxima T_m^i, is plotted in Fig. 2(e). We find that the value of δr_i is constant within the experimental uncertainty and corresponds very well with the thickness of an indium monolayer (i.e., between $a/\sqrt{2} = 2.300$ Å and $c/2 = 2.4735$ Å, where a and c are lattice parameters of tetragonal indium [24]). As a result, it is clear that the periodicity of the oscillations corresponds to the thickness of an atomic layer.

It should be noted that radii of particles are calculated from the planar view TEM micrographs which contain no information about curvature of particles in cross section. Nevertheless, it has been found by comparison of planar views with mass of film that particles can be represented as truncated spheres with a height-to-radius ratio $q = 1.35 \pm 0.15$ [22]. Thus the shape of the particles is invariant over the investigated range of size. The particles grow equally in both lateral and tangential direction and the formation of one additional monolayer on the side of the particle corresponds to the formation of one monolayer on the top of the particle.

The above analysis suggests that within the distribution of particles on the SiN_x surface there is a specific set of particle sizes which are more stable than other particles. The peak-to-peak variation of the caloric response of our measurement can be discussed in terms of cluster stability. We suggest two factors which contribute to the increased heat of melting for stable clusters: (a) stable particles require more heat during melting than clusters of slightly larger or smaller size, and (b) the number of stable clusters on the surface is larger than those of slightly larger or smaller size.

The first factor that contributes to the increase heat of melting for stable clusters is that the stable particles need more heat in order to melt. Such fluctuations have been widely invoked to explain magic numbers in cluster beams [25,26]. Two kinds of magic numbers are commonly considered for metallic clusters. The *electronic* magic numbers, resulting from the interference of the free electron waves in a spherical harmonic potential, are given by $N_e \approx i(i+1)(i+2)/3$. The second kind, the *atomic* or *ionic* magic numbers, correspond to the number of atoms needed to achieve a complete layer of atoms (closed shell) at cluster surface, assuming an icosahedral symmetry. After MacKay [27], they correspond to $N_a = (10i^3 - 15i^2 + 11i - 3)/3$, where i is the shell number.

In order to compare our data with these two models, the number of atoms in the particles corresponding to each maximum T_m^i has been calculated using bulk density of indium and radii according to Eq. (1). A spherical shape of particles is assumed in this case (instead of truncated spheres) in order to compare them with magic numbers, calculated for the nontruncated icosahedral clusters. Results are plotted in Fig. 3, together with the number of atoms corresponding to each magic number model. It is seen that the spacing between our data is very close to the spacing between the atomic magic numbers. However, this result does not imply that the particles actually have icosahedral symmetry. In general, for any crystal shape which can be approximated as a sphere, adding 1 monolayer of atoms to the surface increases the radius by an average thickness of a monolayer.

Figure 3 also shows the irregularity observed by Schmidt *et al.* in calorimetric measurements of the latent heat of melting for sodium clusters by photoabsorption [13], which could be an extension to even smaller particles of the effect reported here.

The second factor which could affect the amplitude of variations in $C_P(T)$ data is the presence of a nonuniform particle size distribution. For the same energetic reasons mentioned previously, the formation of particles with specific sizes may be favored compared to others, resulting in peaks in the $C_P(T)$ curve.

Measurement of the nonuniform size distribution is the means by which stable clusters (magic numbers) are identified in most cluster beam studies [25]. Clusters in our experiment are formed during evaporation and the subsequent annealing through the processes of surface diffusion, Ostwald ripening, and coalescence. No oscillations are observed before annealing while oscillations are observed after annealing. Therefore, there is a reasonable possibility for the formation of a nonuniform size distribution through the process of long range mass transport on the surface.

The most direct way to evaluate the uniformity of particle distribution is by analyzing the distribution data from TEM measurements. However, insufficient resolution of our TEM technique (2–3 Å) and the variation in

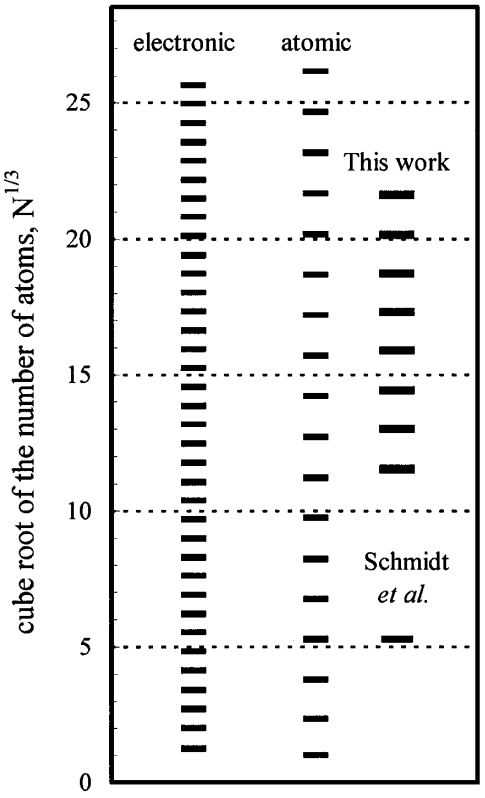

FIG. 3. Number of the atoms corresponding to the size of the particles associated with each melting point maxima T_m^i, in comparison to the *atomic* and the *electronic* magic numbers.

the background of the image due to the SiN_x prevent us from extracting the size of the particles with the required precision.

Finally we estimate the absolute energy associated with the oscillations. Assuming a uniform particle distribution within $\delta r/2$, the heat of melting fluctuates by $\sim$50 eV/particle for particles with T_m from 60 °C (peak) to 65 °C (valley). However, the theoretical estimations of this value were made for only small particles (for atomic shells up to 4th) due to computational difficulties [28,29].

In summary, we have used a sensitive nanocalorimetry technique to investigate the thermodynamic properties of indium cluster formation during the early stages of thin film growth. For the first time, we observe multiple periodic melting peaks in the heat capacity data, which we analyze via the size-dependent melting point depression properties of the indium system. We conclude that there is a certain set of clusters with specific sizes, which are more stable than other sizes. The incremental difference between the sizes of these stable particles corresponds to one atomic layer in radial thickness.

We gratefully acknowledge P. Infante of CNF at Cornell University for assistance in the fabrication of the nanocalorimeters, and L. Hess, D. Cahill, G. Ehrlich, and Joe Greene from the University of Illinois and V. P. Kolesov from the Moscow State University for encouragement in use of the new technique and for useful discussions. This work is supported by the U.S. NSF-DMR 9726458 and 9803019 and ACS-PRF 33580-AC7. Microanalysis characterization was performed at MRL (U.S. DOE), at the University of Illinois, with the assistance of R. D. Twesten, P. D. Miller, and Y. Kim. One of the authors (F. S.) is also grateful to the Canadian NSERC.

*Email address: L-ALLEN9@uiuc.edu

[1] K. N. Tu, J. W. Mayer, and L. C. Feldman, *Electronic Thin Film Science for Electrical Engineers and Materials Scientists* (Macmillan, New York, 1992).
[2] C. V. Thompson, Acta Metall. **36**, 2929 (1988).
[3] J. M. E. Harper *et al.,* MRS Bull. **19**, 23 (1994).
[4] A. Singhal, J. M. Gibson, M. Treacy, P. Lane, and J. R. Shapley, J. Phys. Chem. **100**, 6385 (1996).
[5] R. T. Tung, Appl. Phys. Lett. **68**, 1933 (1996).
[6] S. C. Wang and G. Ehrlich, Surf. Sci. **391**, 89 (1997).
[7] T. P. Martin *et al.,* Chem. Phys. Lett. **172**, 209 (1990).
[8] G. L. Allen *et al.,* Thin Solid Films **144**, 297 (1986).
[9] K. F. Peters, J. B. Cohen, and Y.-W. Chung, Phys. Rev. B **57**, 13 430 (1998).
[10] K. M. Unruh, T. E. Huber, and C. A. Huber, Phys. Rev. B **48**, 9021 (1993).
[11] G. Bertsch, Science **277**, 1619 (1997).
[12] R. S. Berry, Sci. Am. **263**, No. 2, 68 (1990).
[13] M. Schmidt, R. Kusche, B. von Issendorff, and H. Haberland, Nature (London) **393**, 238 (1998).
[14] M. Schmidt, R. Kusche, W. Kronmüller, B. von Issendorff, and H. Haberland, Phys. Rev. Lett. **79**, 99 (1997).
[15] S. L. Lai, J. Y. Guo, V. Petrova, G. Ramanath, and L. H. Allen, Phys. Rev. Lett. **77**, 99 (1996).
[16] J. Knall, J.-E. Sundgren, G. V. Hansson, and J. E. Greene, Surf. Sci. **166**, 512 (1986).
[17] S. L. Lai, G. Ramanath, L. H. Allen, P. Infante, and Z. Ma, Appl. Phys. Lett. **67**, 1229 (1995).
[18] S. L. Lai, G. Ramanath, L. H. Allen, and P. Infante, Appl. Phys. Lett. **70**, 43 (1997).
[19] S. L. Lai, J. R. A. Carlsson, and L. H. Allen, Appl. Phys. Lett. **72**, 1098 (1998).
[20] A. G. Worthing, Phys. Rev. **12**, 199 (1918).
[21] D. W. Denlinger, E. N. Abarra, K. Allen, P. W. Rooney, M. T. Messer, S. K. Watson, and F. Hellman, Rev. Sci. Instrum. **65**, 946 (1994).
[22] M. Zhang, M. Yu. Efremov, F. Schiettekatte, E. A. Olson, A. T. Kwan, S. L. Lai, T. Wisleder, J. E. Greene, and L. H. Allen, Phys. Rev. B (to be published).
[23] Ph. Buffat and J.-P. Borel, Phys. Rev. A **13**, 2287 (1976).
[24] *CRC Handbook of Chemistry and Physics* (CRC Press, New York, 1998), 79th ed.
[25] M. Brack, Rev. Mod. Phys. **65**, 677 (1993).
[26] W. A. de Heer, Rev. Mod. Phys. **65**, 611 (1993).
[27] A. L. Mackay, Acta Crystallogr. **15**, 916 (1962).
[28] H. Cheng and R. S. Berry, Phys. Rev. A **45**, 7969 (1992).
[29] R. B. McClurg, R. C. Flagan, and W. A. Goddard, J. Chem. Phys. **105**, 7648 (1996).